Tetrahedron 67 (2011) 7392–7399

Contents lists available at ScienceDirect

Tetrahedron

journal homepage: www.elsevier.com/locate/tet

Thiacalix[4]arene–alkali metal assemblies: crystal structures and guest-binding capabilities of supramolecular architectures supported by metal coordination and cation–π interactions

Manabu Yamada [a], Yoshifumi Shimakawa [b], Fumio Hamada [b,*]

[a] Venture Business Laboratory, Akita University, Akita 010-8502, Japan
[b] Department of Material-Process and Applied Chemistry for Environments, Faculty of Engineering and Resource Science, Akita University, Akita 010-8502, Japan

ARTICLE INFO

Article history:
Received 25 May 2011
Received in revised form 11 July 2011
Accepted 11 July 2011
Available online 20 July 2011

Keywords:
Calixarenes
Thiacalixarenes
Alkali metal complexes
Crystal structures
Guest-binding properties

ABSTRACT

To investigate alkali metal complexation with sulfur-linked calixarene analogues and their guest-binding properties for gaseous organic guest molecules, we elucidated a crystal structure of a cesium complex with *p*-H-thiacalix[4]arene (**1**·4H) ligands and guest-binding properties of the cesium complex (**2**) and the previously reported rubidium complex (**3**). In crystals of the complex **2**, a 'sandwich-like' binuclear complex was formed by inter-molecular coordination of cesium cations to the thiacalixarene molecules and methanol molecules, mutually interacting by aromatic-H···S hydrogen bonding and alkali metal cation–π interactions between the alkali metal cation and thiacalixarene aromatic rings outside of the cavities. On the guest-binding behaviors both complexes **2** and **3** toward organic guest molecules, methanol, ethanol, and 1-propanol as polar molecules, the complex **2** has no methanol adsorption ability, but the complex **3** showed vapor adsorption properties for all guest molecules. In particular, both complexes exhibited a high adsorption capability toward ethanol molecule. As results of gaseous guest adsorption measurements for alcohol molecules, the guest-binding of these complexes are significantly different because the properties depend heavily on structural natures between complexes **2** and **3**.

1. Introduction

Since the facile synthetic methods of the parent calixarenes as an artificial receptor had been pioneered by Gutsche, the functions of calixarenes have been studied, such as the guest-binding toward many organic components and metal-complexation for metal ions in supramolecular chemistry, as well as those of crown ethers and cyclodextrins.[1] On the other hand, considerable attentions have been focused on thiacalixarenes as the interesting molecular building blocks because of their intriguing properties and their increased versatility over calixarenes.[2] Thiacalixarenes are comprised of phenol units linked with elemental sulfurs, where bridging methylene moieties of the parent calixarenes are completely replaced by sulfide moieties. Therefore, they could be suited for infinite inter-molecular interactions in the crystalline state because their bridging sulfur moieties are capable of both hydrogen bonding and metal coordination extensively. In relation to this, the chemistry of thiacalixarenes has thus far been revealed that they have the significant capabilities toward a wide range of metal ions, such as selective metal coordination,[3] chelating effect,[4] and chemical sensing.[1e,5] To date, alkali metal cation coordination chemistry involving calixarenes and thiacalixarenes have been intensively investigated in selective extraction capabilities for alkali metal cations by the use of the corresponding derivatives as extraction regents.[1,3] In addition, structural studies of alkali metals Li–Cs complexes in the solid state are conducted because alkali metals play a prominent role in synthesizing thia- and calixarenes, and particular thia- and calixarenes exhibit selective complexation with alkali metal ions in alkali metal coordination.[6–8] However, few structural studies of thiacalixarene complexes with alkali metals have been reported. First, X-ray crystallographic analysis of *p*-^{t}Bu-thiacalix[4]arene complexes with alkali metals Li to Cs have been published by Harrowfield and co-workers.[7] In the cases of alkali metal Li–Cs complexes, *p*-^{t}Bu-thiacalix[4]arene ligands are partially deprotonated. These metal cations interacted with the bridging sulfur atoms and the pendent phenolic/phenoxide oxygen donor atoms belonging to the thiacalixarene ligands. Similarly, Zeller and Radius have reported that *p*-^{t}Bu-thiacalix[4]arene ligand formed full deprotonation by using *n*-BuLi, NaH, and KH as strong bases in the Li to K cluster complexes.[8] Recently, we have shown that X-ray crystal structures of potassium metal complexes with *p*-^{t}Bu-thiacalix[4/6/8]arenes constructed supramolecular assemblies by inter-molecular

* Corresponding author. Tel.: +81 18 889 2440; fax: +81 18 837 0404; e-mail address: hamada@ipc.akita-u.ac.jp (F. Hamada).

0040-4020/$ – see front matter © 2011 Elsevier Ltd. All rights reserved.
doi:10.1016/j.tet.2011.07.027

hydrophobic interactions and metal coordination between the pendent phenolic/phenoxide oxygen atoms and bridging sulfur atoms belonging to their thiacalixarene ligands.[9] In addition, these assemblies indicated that both a 'non-porous' structure in the thiacalix[4]arene complex and 'zeolitic-porous' structures in the thiacalix[6/8]arenes complexes have been strongly influenced by hydrophobic interactions of their ^{t}Bu-moieties in the crystalline states. With this in mind, we further revealed that these assemblies were capable of crystalline phase guest-addition and -removal for vapor organic molecules, such as methanol, ethyl acetate, and benzene. Despite the 'non-porous' structure of *p*-^{t}Bu-thiacalix[4]arene–potassium complex, the complex showed a unique adsorption behavior for organic gaseous molecules. The guest-binding properties of *p*-^{t}Bu-thiacalix[6/8]arenes–potassium complexes that possessed the 'zeolite-like' structures naturally exhibited the adsorption capabilities of vapor organic guest molecules.

Generally, interactions between alkali metal ions and calixarene analogues have been observed by alkali metal cations coordinated to the pendent phenolic/phenoxide oxygen atoms of the calixarenes, or alkali metal cations are included into calixarene analogue cavities in the chemistry of calixarenes.[6] The metals in the latter phenomenon are stabilized by alkali metal cation–π interactions in the cavities, although there is a study describing the occurrence of the alkali metal cation–π interaction between *p*-H-calix[4]arene aromatic rings outside of cavities and potassium cations in the crystalline state.[6d] More recently, we have also demonstrated that alkali metal complexes based on *p*-H-thiacalix[4]arene ligand exhibited two types of alkali metal cation–π interactions: alkali metal cation–π interactions in the *p*-H-thiacalix[4]arene cavities and at *p*-H-thiacalix[4]arene aromatic rings outside of cavities from single-crystal X-ray diffraction studies.[10] In the case of the potassium complex with *p*-H-thiacalix[4]arenes and *n*-butanols, eight potassium cations indicated two triangular pyramidal arrangements, which are bridged at planar phenoxide oxygen atoms and linking sulfur atoms belonging to the thiacalixarene ligands further supported by alkali metal cation–π interactions of η^1 and η^6 coordination in the thiacalixarene cavities.[10b] By contrast, the rubidium complex with the thiacalixarene ligand has shown that the two types of alkali metal cation–π interactions of η^2 and η^6 coordination based on two different molecular units of *p*-H-thiacalix[4]arene molecules were observed at *p*-H-thiacalix[4]arene aromatic rings outside of cavities.[10a] As mentioned above, if there are no ^{t}Bu-moieties at the *para*-positions of the thiacalixarenes, the construction of a renewed supramolecular assembly could be expected by intra- and inter-molecular interactions.

From this point of view, we explored how *p*-H-thiacalix[4]arene ligand (**1**·4H, Scheme 1) behaves toward the cesium larger than those potassium and rubidium in the crystalline state, providing further insights on guest-binding properties of alkali metal complexes for alcohol molecules. Herein we describe a structural comparison with the cesium complex (**2**) and the rubidium complex reported previously (**3**), and report guest-binding properties of both complexes for alcohol molecules.

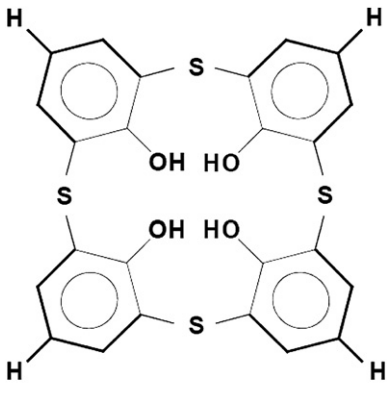

1·4H

Scheme 1. Structural formula of *p*-H-thiacalix[4]arene (**1**·4H).

2. Experimental section

2.1. Physical measurements

IR spectra were measured by using KBr disks with a Perkin–Elmer SPECTRUM 2000 spectrophotometer. ^{1}H NMR spectra were taken on a Bruker DPX 300, and measured using tetramethylsilane as an internal standard and CD_3OD as a solvent, unless otherwise noted. Microanalyses were performed at the microanalysis center of Tohoku University. The binding isotherms were obtained with a BELSORP 18 automated gas adsorption apparatus. Powder X-ray diffractions (PXRD) were collected with a Rigaku Ultima IV diffractometer by using Cu Kα radiation (λ=1.5406 Å, 40 kV, 40 mA) with a graphite monochrometer at a step width of 0.02° 2θ and a scan speed 2.000° min^{-1}. Thermogravimetric analysis (TGA) was recorded on a Rigaku Thermo Plus TG 8120 apparatus in the temperature range between 30 and 600 °C under a nitrogen atmosphere at a heating rate 10 °C min^{-1}.

2.2. Materials

All reactions were carried out in nitrogen atmosphere. Tetrahydrofuran (THF) was distilled from sodium/benzophenone under nitrogen and stored over 4 Å activated molecular sieves. Methanol was commercially available and used as recrystallization solvent without further purification. *p*-H-Thiacalix[4]arene (**1**·4H) was obtained by de *tert*-butylation reaction from *p*-^{t}Bu-thiacalix[4]arene,[11] which was prepared according to our previously reported procedures.[12] Methanol and ethanol were distilled from iodine/magnesium under nitrogen, and 1-propanol was refluxed over and then distilled from CaH_2 under nitrogen before use of vapor adsorption measurements.

2.3. Synthesis of [Cs(1·3H)]$_2$·2MeOH complex (2)

To a suspension of **1**·4H (0.5 g, 1.01 mmol) in THF (30 mL) added Cs_2CO_3 (3.28 g, 10.1 mmol), and a white suspension was obtained. The reaction mixture was stirred and refluxed for 24 h under nitrogen atmosphere. After cooling down to ambient temperature, all the solvent was removed in vacuo. Excess Cs_2CO_3 of the reactants was dissolved with water, and the resulting white precipitates were collected by filtration with glass filter. The precipitates were washed three times with water, dried under vacuum overnight at 150 °C. The resulting solid material was dissolved in methanol (300 mL) and remained insoluble matter was filtered out. The clear solution thus obtained was allowed to stand for about 2 weeks to afford colorless block crystals of the adduct (0.32 g, 48% yield): IR (KBr): ν 3416, 3360 (O–H), 1441 (C=C), 1253 (C–O) cm^{-1}. ^{1}H NMR (300 MHz, CD_3OD, 25 °C, TMS): δ 7.32 (d, 8H, Ar–H), 6.38 (t, 4H, Ar–H). Anal. Calcd for $[Cs(\mathbf{1}\cdot 3H)]_2\cdot 2H_2O$=$C_{48}H_{30}O_8S_8Cs_2\cdot 2H_2O$: C, 44.62; H, 2.65. Found: C, 44.95; H, 2.95. FABMS *m*/*z* 760.8 ([M]$^{2+}$, calcd 760.6).

2.4. Crystal structure determination of complex 2

The crystals containing mother liquor were drunk up with a pipette, which dropped in paraffin oil. Single crystals coated with the oil were picked up with on MicroMounts™, and the crystals were placed immediately in a cold nitrogen stream at −173 °C. X-ray

diffraction data for complex **2** was collected on a Rigaku PAXIS RAPID imaging plate diffractometer with a graphite monochromated Mo Kα radiation (λ=0.71075 Å). The structure was solved by direct methods using SHELXS-97[13] and refined by full-matrix least-squares on F^2 using the SHELXL-97[14] program. The non-hydrogen atoms were refined anisotropically. Hydrogen atoms of aromatic rings and methyl group of the coordinated methanol molecules in complex **2** were calculated, and all hydrogen atoms of hydroxyl groups found from the residual density and refined.

2.4.1. Crystal data for complex ***2****.* $C_{50}H_{38}O_{10}S_8Cs_2$, M=1321.14, colorless block, crystal dimensions 0.30×0.25×0.20 mm, monoclinic, space group $P2_1/n$, a=13.3830(7), b=10.8649(5), c=18.3500(9) Å, β=112.5895(10), V=2463.5(2) Å^3, Z=2, Mo Kα radiation (λ=0.71075 Å), D_{calcd}=1.781 g cm^{-3}, T=100 K, μ(Mo Kα)=21.659 cm^{-1}, 30,899 measured reflections, 9722 unique reflections (R_{init}=0.048), 6035 observed reflections ($I>2.00\sigma(I)$), 317 parameters, R=0.0239, wR=0.0511, refined against $|F|$, GOF=1.049. Crystallographic data of the crystals have been deposited at the Cambridge Crystallographic Data Center in CIF format CCDC no. 722469. Copies of the data can be obtained free of charge on application to CCDC, 12 Union Road, Cambridge CB2 1EZ, UK (e-mail: deposit@ccdc.cam.ac.uk).

2.5. Vapor adsorption measurements for complexes 2 and 3

The binding isotherms were obtained with a BELSORP 18 automated gas adsorption apparatus. In the sample chamber (ca. 15 mL) maintained at 25.0±0.1 °C was placed guest-free crystals of each complex, which has been pretreated at 100 °C (in the case of complex **2**) or 60 °C (in the case of complex **3**) at <10^{-3} Torr. The larger gas chamber (176.36 mL) with a pressure gauge was kept at 50±0.1 °C. Helium gas at certain pressure was introduced in the gas chamber and was allowed to diffuse into the sample chamber by opening a valve. The change in pressure allowed an accurate determination of volume of the total gas phase. Host–guest complexation was monitored in a similar manner by using a guest vapor in place of helium. The amount of guest adsorbed was calculated readily from the pressure difference ($P_{calcd}-P$), where, P_{calcd} is the calculated pressure if there were no guest adsorption, as in the case of helium, and P is the observed equilibrium pressure, as which the change in pressure in 300 s had become smaller than 1% of the pressure at the point. All operations were computer-controlled and automatic. The specific surface areas (A_{BET}) were obtained by using the same apparatus. The adsorption isotherm for N_2 at 77 K (Supplementary data Figs. S2 and S3) cannot fit well with BET equation, $P/V(P-P_s)=1/V_mC+[(C-1)/V_mC](P/P_s)$, where P_s is saturation vapor pressure of N_2 at 77 K and is 760 Torr, V (mL/g) is the amount (in terms of volume in the standard state) of N_2, adsorbed per gram of adsorbent, V_m is that for saturation monolayer coverage, and C is a constant.

3. Results and discussion

3.1. Crystal structure of the cesium complex with the thiacalixarene ligands

The reaction of **1**·4H with 10-fold excess of cesium carbonate in THF, followed by recrystallization from methanol solution, grew upon crystals as colorless blocks of [Cs(**1**·3H)]$_2$·2MeOH (**2**) complex. The asymmetric unit of this complex comprised one independent molecule of the thiacalix[4]arene ligand and one cesium cation that is coordinated to one methanol molecule. The thiacalixarene ligand chelating through a pair of adjacent pendent phenolic/phenoxide oxygen atoms together with one bridging sulfur atom adopts the pinched cone-like conformation. The resulting complex **2** crystallized in the space group $P2_1/n$ and Z=2 with an overall composition [{thiacalix[4]arene$^-$}$_2${cesium$^+$}$_2$(MeOH)$_2$]. Charge neutrality dictates the thiacalix[4]arene is in mono-anion form. The X-ray crystal structure of the 1:1 complex of cesium with the thiacalixarene constructed a 'sandwich-like' binuclear dimer, i.e., two thiacalixarene molecules sandwich two cesium cations and two methanol molecules (Fig. 1).

The conformation of the thiacalixarene molecule is maintained by two OH···O intramolecular hydrogen bonding between phenolic hydroxyl hydrogen atoms and phenoxide oxygen atom with the distances 1.717 and 1.860 Å (corresponding O···O distances 2.572 and 2.594 Å, Fig. 1b). By contrast, the other phenolic hydrogen atom interacted with the coordinated methanol hydroxyl oxygen atom and the linking sulfur atom of the PhOH(14)···O(5)Me distance 2.460 Å (corresponding O(3)···O(5) distance 3.010 Å) and the PhOH(14)···S(3) distance 2.525 Å (corresponding O(3)···S(3) distance 2.997 Å). With this unit, the dimeric structure of the 'sandwich-like' fashion was provided by the coordination of cesium cations to pendent phenolic/phenoxide oxygen atoms and linking sulfur atoms belonging to thiacalixarene ligands (Table 1).

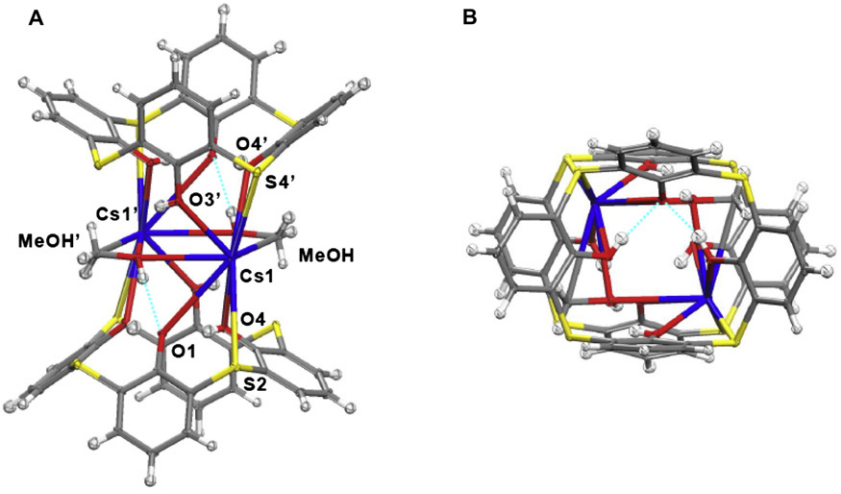

Fig. 1. The crystal structure of complex **2** showing (A) side view of thiacalix[4]arene complex with cesium cations and methanol molecules, (B) top view of intramolecular hydrogen bonding between hydroxyl groups of thiacalix[4]arene ligands. Conventional atom colors of carbons, oxygens, sulfurs, cesiums, and hydrogens in complex **2** are in gray, red, yellow, blue, and white, respectively.

Table 1
Selected bond lengths and angles (Å and °) for complex **2**

Cs(1)–O(1)	3.619	O(1)–Cs(1)–O(4′)	139.08
Cs(1)–O(2)	3.397	O(3′)–Cs(1)–O(4′)	64.60
Cs(1)–O(3′)	2.930	S(2)–Cs(1)–O(1)	48.09
Cs(1)–O(4′)	3.151	S(2)–Cs(1)–O(2)	51.63
Cs(1)–S(2)	3.726	S(2)–Cs(1)–O(3′)	127.39
O(1)–Cs(1)–O(2)	43.26	S(2)–Cs(1)–O(4′)	167.56
O(1)–Cs(1)–O(3′)	99.68	O(5)–Cs(1)–O(5′)	82.93

The prime denote inversion related. Symmetry transformations used to generate equivalent atoms: ′, 2–*x*, 1–*y*, 2–*z*.

The binuclear dimer was further supported by two methanol molecules that are maintained via inter-molecular metal coordination between methanol hydroxyl oxygen atoms and cesium cations, and also inter-molecular hydrogen bonding between the hydroxyl hydrogen atoms of methanol molecules and phenoxide oxygen atoms of each thiacalix[4]arene ligand. When comparing the crystal structure of the complex **2** with that of the previously reported rubidium complex **3**, each metal coordination environment toward the thiacalixarene ligand is significantly different. Although the formation of 'sandwich-like' dimeric structures was adopted in both complexes **2** and **3**, two cesium cations bind to all four oxygen atom of the thiacalix[4]arene ligands in complex **2**. In the case of complex **3**, two rubidium cations, however, associated with three or four oxygen atom between thiacalixarene skeletons that existed as partially or fully coordination of rubidium cations to phenolic/phenoxide oxygen atoms. This means the different location between the cesium and rubidium on thiacalixarene ligands has an obvious effect on the distinct behaviors of both structures in complexes **2** and **3**, and hence a comparison of the Cs–Cs distance in complex **2** with the Rb–Rb distances in complex **3** is remarkable difference (the distance is 4.886 Å in complex **2**, and the distances are 4.392 and 4.573 Å in complex **3**, respectively). In addition, both complexes have predominant influences on methanol as guest molecules during the formation of 'sandwich-like' dimeric structures. The guest molecules of complex **2** were captured between two thiacalixarene ligands and further supported by OH···O hydrogen bonding between methanol hydroxyl groups and thiacalixarene phenoxide oxygen atoms (the corresponding OH(19)···O(1′) distance 2.029 Å) and metal coordination between methanol molecules and cesium cations (the corresponding Cs(1)···O(5) distance 3.288 Å and Cs(1)···O(5′) 3.232 Å), whereas those of complex **3** only coordinated to rubidium cation and were not captured between thiacalixarene ligands on the lower rims. Comparison to the structures of alkali metal salts with thia- and calix[4]arenes, the current resulted 'sandwich-like' dimeric structure of complex **2** as a binuclear complex resembles in methylene-linked calix[4]arene-alkali metal complexes[6d,e] and the previous crystal structures of *p*-^{t}Bu-thiacalix[4]arene–potassium complexes[7,9c] rather than the intricate coordination environments between four *p*-^{t}Bu-thiacalix[4]arene molecules and three cesium ions in the crystal structure of *p*-^{t}Bu-thiacalix[4]arene–cesium complex published by Harrowfield and co-workers.[7] Interestingly, a surprising feature in complex **2** provides further evidence between the captured methanol molecules and the cesium cations in the binuclear dimer where are observed close methyl···Cs distances between the methyl groups of solvated methanol molecules and cesium cations. The metal cations may be coordinated to methyl group of the solvated molecules with the C···Cs distance of 3.435 Å, and the close C–H···Cs distances are also observed between methyl group of the guest molecules and cesium cations with 3.166 and 3.264 Å, respectively. The close C···Cs and C–H···Cs interactions might be occurred in crystal packing, but the fact existed as the important interaction of cesium cations with methanol molecules to construct the dimer formation in the complex **2**.

In extended structure of the complex, the dimers form layer structures by the thiacalix[4]arene cavity of the base dimer includes into one aromatic ring of a nearest adjacent dimer, and the layer structures are stabilized by two π–π interactions at face-to-face and edge-to-face positions through the inclusion of the base thiacalix[4]arene aromatic ring within the inversion-related cavity of the nearest adjacent thiacalix[4]arene ligand (the face-to-face distance of 3.643 Å and the edge-to-face distances of 2.868 and 3.237 Å, respectively, Fig. 2).

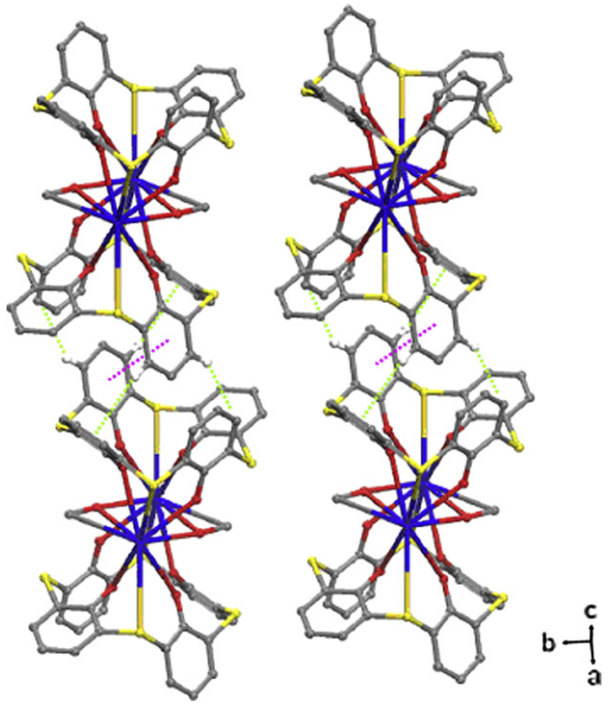

Fig. 2. The layer formation by two π–π interactions of face-to-face and edge-to-face through the inclusion of the base thiacalix[4]arene aromatic ring within the inversion-related cavity in complex **2** (pink and green dotted lines).

Moreover, it is recognized to be involving the thiacalix[4]arene unit in two different directions in the extended structure of the layers, but both the thiacalix[4]arene structures adopted same conformation when viewed along with [011] plane (Fig. 3).

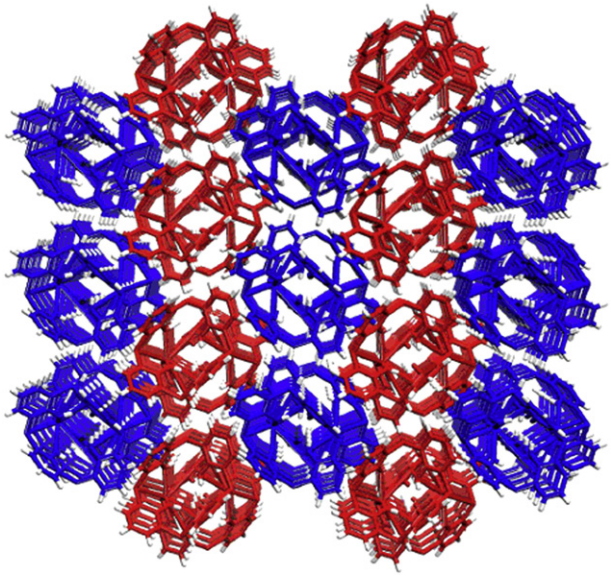

Fig. 3. The overall crystal structure showing alternately stacking of two different directional layers when viewed along with [011] plane.

The interaction between layers are observed in inter-layer interactions of aromatic-H···S hydrogen bonding and an alkali metal cation–π interaction of η^2 coordination between the base thiacalix[4]arene layer and the nearest adjacent thiacalixarene layer (the aromatic-H···S distances ranging from 2.688 to 3.153 Å and the cation–π distances of 3.588 and 3.601 Å, respectively, Fig. 4).

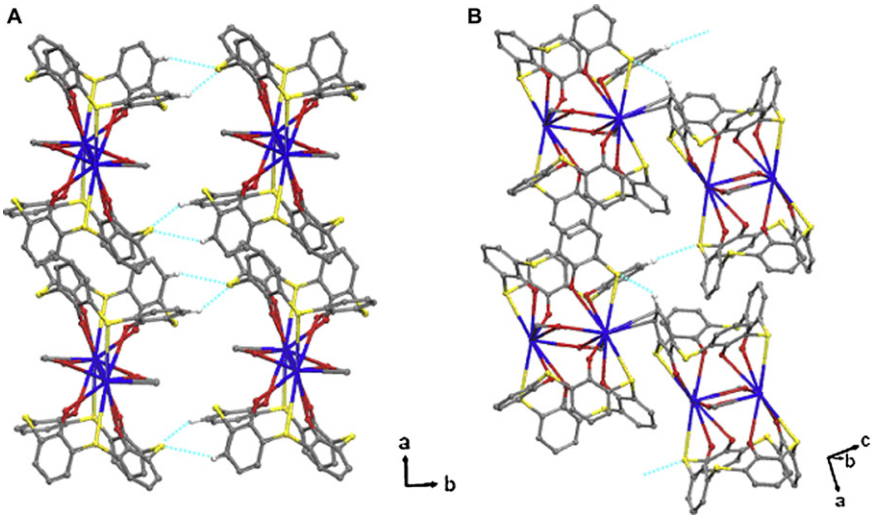

Fig. 4. Extended structures of layers in complex **2** showing (A) aromatic-H···S hydrogen bonding between same directional layers (light blue dotted line), (B) the alkali metal cation–π interaction of η^2 coordination and the aromatic-H···S hydrogen bonding between different directional layers (light blue dotted lines).

In contrast, the extended structure of complex **3** has been observed either an alkali metal cation–π interaction or aromatic-H···S hydrogen bonding in each inter-layer. In other words, the different phenomena between each complex are occurred by the location and intermetallic distances of each metal on the 'lower-rim' of thiacalix[4]arene ligands in these cases. As mentioned above, these results illustrate important roles to form the supramolecular architecture of complex **2** by intra- and inter-molecular interactions, such as alkali metal cation–π interactions, metal coordination bonds, and hydrogen bonding. Furthermore, it might be suggested that the behavior of cesium cations toward thiacalix[4]arene ligands and the intermetallic Cs–Cs distances play a dominant role in important factors to obtain the intriguing architecture.

3.2. The guest-binding properties of the cesium complex (2) and the rubidium complex (3)

To investigate the structural stabilities of complexes **2** and **3** during desolvation process, we carried out thermogravimetric analysis (TGA). Upon heating the crystals **2** and **3** complexes, the thermal stabilities of both complexes were observed different behaviors (Fig. 5).

In the case of complex **2**, the crystals showed a gradual loss of weight to reach a constant value at 170 °C, and then decomposed above 310 °C in stages. The obtained overall weight change of **2** was ca. 5.4% loss of weight during desolvation process in the first stage, which is equivalent to the all loss of two methanol molecules per one dimeric structure in crystals **2**. In contrast, the complex **3** immediately loses methanol molecules of its crystals at the beginning of thermogravimetric analysis, which indicates the escape of the methanol molecules from crystals **3** at room temperature. The weight of the crystals were gradually decreased to reach a constant value at 150 °C, and then decomposed above 310 °C in stages. The observed overall weight change of **3** was ca. 8.1% loss of weight during desolvation process in the first stage, which could not fit well with calculated value of the all loss of four methanol molecules because the coordinated methanol molecules of the complex **3** are easily-removable by exposing to air from the mother liquor. The different desolvation processes between complexes **2** and **3** attribute to the coordination environments of cesium or rubidium to methanol molecules and the location of methanol molecules in each sandwiched dimer as results of single-crystal X-ray analysis. Likewise, both complexes **2** and **3** were also feasible to desolve via heating treatments of the crystals **2** at 100 °C under 10^{-3} Torr and the crystals **3** at 60 °C under 10^{-3} Torr.

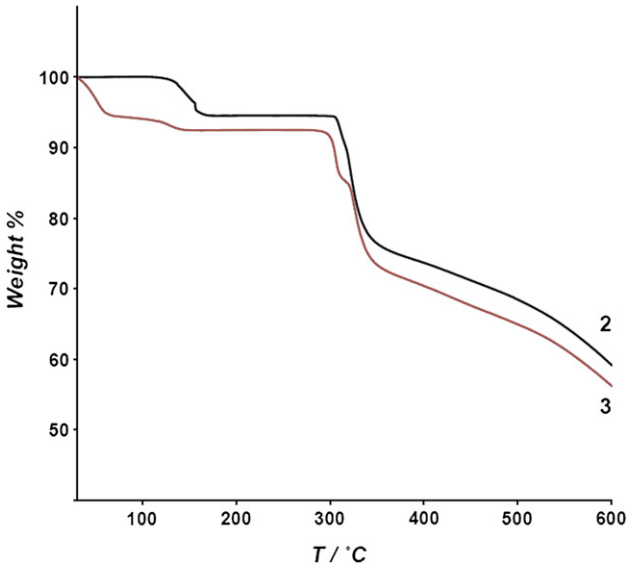

Fig. 5. Thermogravimetric analysis (TGA) of complexes **2** (black line) and **3** (red line) recorded in the temperature range between 30 and 600 °C under a nitrogen atmosphere at a heating rate 10 °C min^{-1}.

In addition, to examine the microcrystalline states and the crystalline phase guest-binding properties of the methanol-free crystals **2** and **3**, we also investigated powder X-ray diffraction (PXRD) and vapor adsorption studies by using the complete methanol-free crystals of the complexes **2** and **3** that were prepared according to the above heating treatments under reduced pressure. The methanol-free crystals of both complexes are microcrystalline materials as evidenced by their PXRD patterns (Supplementary data Fig. S1). The PXRD pattern of the methanol-free crystals **2** fitted with the calculated PXRD patterns from crystal structure of the original adduct. The methanol-free crystals **2** is a microcrystalline material with the close

structure of the original adduct during the desolvation process of guest molecules, indicating that the supramolecular assembly has robust and stable structure because the PXRD patterns are similar with each other. In contrast, the PXRD pattern of the guest-free crystals **3** slightly disagreed with the calculated PXRD patterns from crystal structure of the original adduct. Although the methanol-free crystals **3** are a microcrystalline material, the behavior probably showed that the crystal structure slightly changed during the desolvation process, owing to easily-removable methanols from the crystal lattice. Subsequently, the small specific surface areas A_{BET} of the microcrystalline materials **2** and **3** could not be obtained by an adsorption isotherm for N_2 at 77 K, because of structural natures by desolvating the coordinated guest molecules from their crystal lattices, which indicate that the cavities of the assemblies **2** and **3** are slightly shrunk to be unable to adsorb N_2 (Supplementary data Figs. S2 and S3). However, the most striking features in the guest-free crystals **2** and **3** are that both shrunk structures exhibited the guest-binding properties toward three alcohol molecules of methanol, ethanol, and 1-propanol by vapor adsorption studies (Figs. 6 and 7).

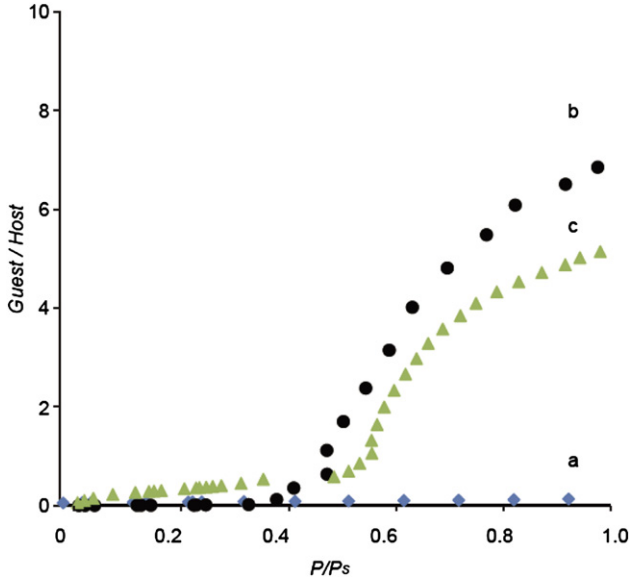

Fig. 6. Binding isotherms for gaseous methanol (a, ◇), ethanol (b, ○), and 1-propanol (c, △) at 25 °C with the guest-free crystals **2**.

Binding isotherms for vapor organic guests were recorded on the methanol-free crystals **2** and **3**, where the molar ratio of the guests bound to microcrystalline **2** and **3** used are plotted against the guest pressure at 298 K for the adsorption. On the adsorption of the guest-free crystals **2** toward each guest alcohol molecule, although the guest-binding for methanol as the original guest could not be observed, the guest-free crystals **2** have a capture of ethanol and 1-propanol molecules. In the comparison of adsorbed amounts between ethanol and 1-propanol, the guest-free crystals **2** have shown higher adsorption capability of ethanol molecules than that of 1-propanol molecules. In detail, the adsorption of each alcohol molecules is as follows. In the case of the ethanol adsorption, the guest-free crystals **2** gave rise to almost no uptake of gaseous ethanol molecules up to ca. 0.5 P/P_s, and then the ca. six guest molecules per the dimer were rapidly adsorbed on the guest-free crystals **2** within the saturation pressure (P_s=7.85 kPa). On the 1-propanol adsorption, the guest-free crystals **2** could gradually capture the gaseous guest molecules up to ca. 0.5 P/P_s. After that, rapid uptake of ca. five guest molecules per the dimer by the guest-free crystals **2** was found within the saturation pressure (P_s=2.72 kPa). This might be suggested that the guest-free crystals **2** showed similar adsorption

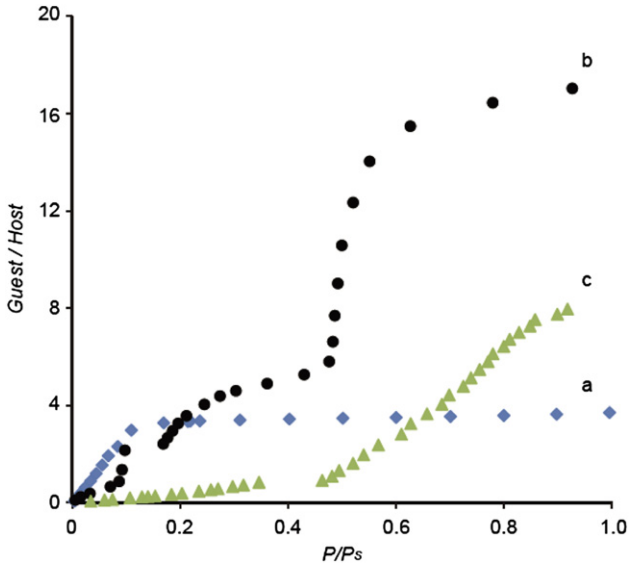

Fig. 7. Binding isotherms for gaseous methanol (a, ◇), ethanol (b, ○), and 1-propanol (c, △) at 25 °C with the guest-free crystals **3**.

behaviors and characteristic of guest-induced phase changes at ca. 0.5 P/P_s during the guest vapor adsorption processes. By contrast, the different guest-binding properties of the methanol-free crystals **3** become evident in adsorption experiments with three alcohol molecules compared to that found in the crystals **2**. The crystals **3** were able to absorb all gaseous guest molecules, indicating that adsorption ability of crystals **3** possessed higher adsorbed amount of guest ethanol molecules than those of other guest alcohol molecules. On the adsorption of methanol as an original guest at above 0.1 P/P_s, rapidly, ca. four methanol molecules per the dimer gave rise to uptake into the crystals **3**, and then the amount of adsorption was a constant up to the saturation vapor pressure (P_s=16.939 kPa). This methanol adsorption result of the crystals **3** suggests that the guest-induced crystals might regenerate the original crystal structure of **3** during the methanol adsorption of original guests. Surprisingly, the crystals **3** showed four-step adsorption in the case of ethanol adsorption. Although the crystals gradually sorbed the vapor ethanol molecules at ca. 0.5 P/P_s, ca. 16 ethanol molecules per the dimer were rapidly captured into the crystals within the saturation pressure. On the other hand, the guest-binding for 1-propanol molecules was shown that ca. six molecules increasingly sorbed into the dimer of crystals **3** within the saturation pressure. The selective adsorption properties of the vapor guests might be educed by characteristic of guest-induced phase changes and the structural nature of the crystals **3** because of slight translations of the crystal structure during the methanol desolvation process. As results of the guest-binding properties of these crystals for three molecules, both crystals **2** and **3** showed the highest adsorption ability for vapor ethanol as a guest molecule in three alcohol molecules. When comparing the guest-binding of the crystals **2** with that of the crystals **3**, the different behaviors toward three alcohol molecules were observed between the crystals **2** and **3**. As mentioned above, the most reasons may suggests that the crystal structures **2** and **3** have much effect on the different metal coordination environments and the location of guest methanol molecules between the thiacalixarene ligands in these crystalline states. Thus, the behaviors are decided whether to retain stable or to release easily methanol as the solvate molecule in both crystals **2** and **3** because the vapor guest adsorption sites of both crystals might be occurred at the places of the removed original methanol guests.

To elucidate varying crystal structures of the crystals **2** and **3** by the guest-binding properties of three alcohol molecules, we

measured their PXRD patterns of immediate after the vapor adsorption experiments.

Although the PXRD pattern of the guest-free crystals **2** (a) displays a similarity to the PXRD pattern of the crystals **2** after methanol adsorption (b), the PXRD patterns between the guest-free crystals (a) and the crystals after ethanol and 1-propanol adsorptions (c and d) revealed appreciable changes (Fig. 8). In the case of the crystals **3**, same behaviors of the crystal **2** for the guest molecules are also observed in the crystals **3**. The similar PXRD patterns found between the guest-free crystals **3** (a) and the crystals **3** after methanol adsorption (b), and the different PXRD patterns exist between the guest-free crystals (a) and the crystals after ethanol and 1-propanol adsorption (c and d) (Fig. 9).

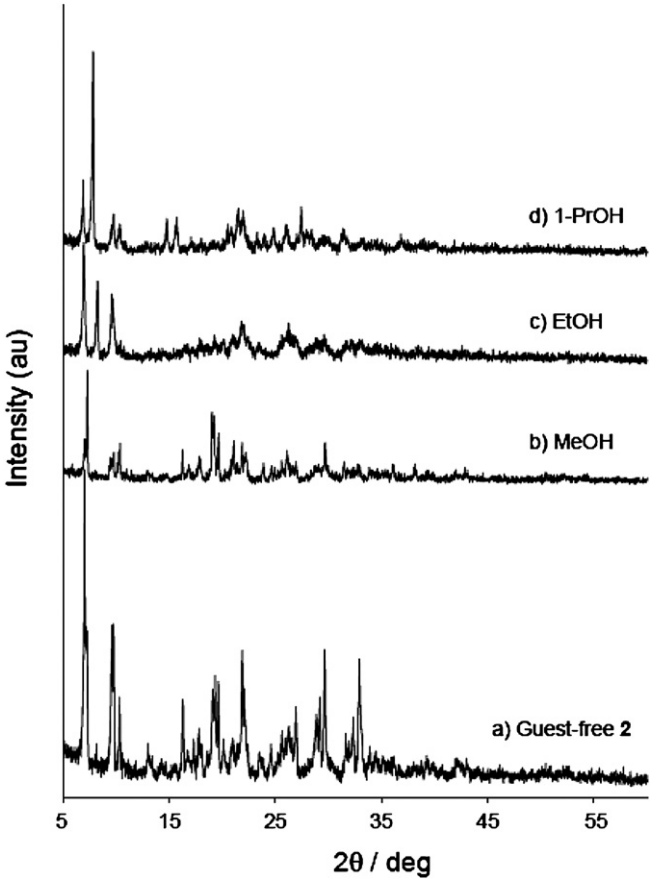

Fig. 8. (a) Powder X-ray diffraction (PXRD) patterns for guest-free crystals **2**. (b) PXRD patterns for immediate after the methanol adsorption experiments of guest-free crystals **2**. (c) PXRD patterns for immediate after the ethanol adsorption experiments of guest-free crystals **2**. (d) PXRD patterns for immediate after the 1-propanol adsorption experiments of guest-free crystals **2**.

From the PXRD experimental results, it is probable that both guest-free crystals **2** and **3** can discriminate the size of three alcohol molecules and change to accommodate themselves to the guest molecules during the guest-binding processes.

4. Conclusions

We have demonstrated the crystal structure of the binuclear complex **2** that are formed from the reaction of cesium carbonate and *p*-H-thiacalix[4]arene (**1**·4H) and the guest-binding properties of guest-free complexes **2** and **3** toward methanol, ethanol, and 1-propanol as polar molecules. X-ray crystallographic analysis has revealed that the crystal structure constructed a 'sandwich-like'

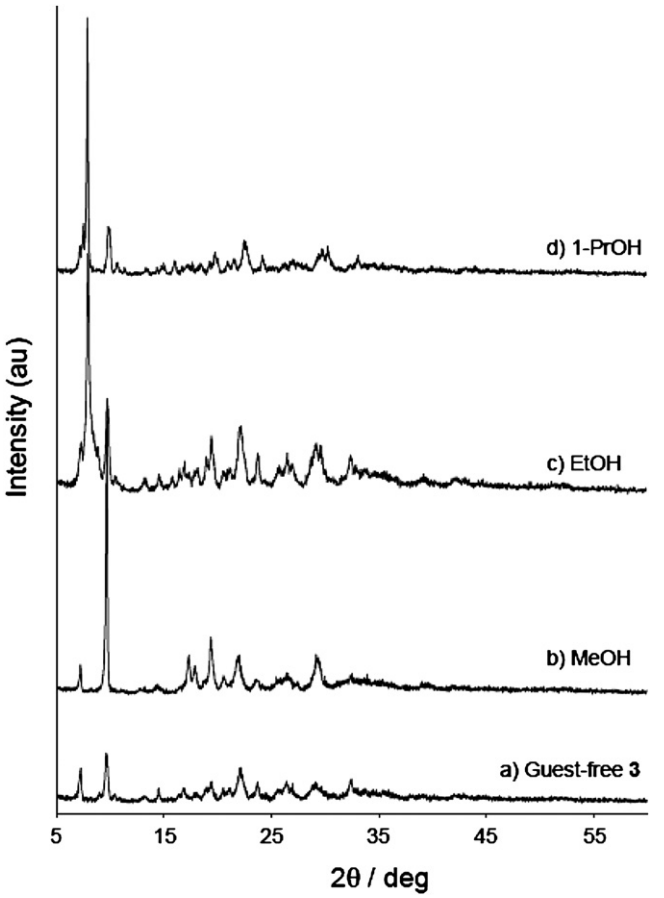

Fig. 9. (a) Powder X-ray diffraction (PXRD) patterns for guest-free crystals **3**. (b) PXRD patterns for immediate after the methanol adsorption experiments guest-free crystals **3**. (c) PXRD patterns for immediate after the ethanol adsorption experiments of guest-free crystals **3**. (d) PXRD patterns for immediate after the 1-propanol adsorption experiments of guest-free crystals **3**.

binuclear dimer, which composed of two thiacalixarene molecules, two cesium cations, and two methanol molecules. The layer structures based on the 'sandwich-like' dimers through two π–π interactions mutually interacted by the aromatic-H···S hydrogen bonding and the alkali metal cation–π interactions between the inter-layer structures to establish the supramolecular architecture. The coordination environments between complexes **2** and **3** are somewhat different because the phenomena are occurred by the location and intermetallic distances of each metal on the 'lower-rim' of thiacalix[4]arene ligands, indicating that thermal stabilities of crystals **2** and **3** have an effect on desolvation processes of methanol molecules from crystals **2** and **3** by TGA measurements. After desolvation, the microcrystalline material **2** indicated the similar structure of the original adduct **2**, but the microcrystalline material **3** disagreed with the original adduct **3** because the crystal structure slightly changed during the desolvation process as shown by powder X-ray diffraction studies. On the other hand, the resultant microcrystalline materials **2** and **3** were capable of adsorbing volatile alcohol molecules except methanol adsorption of the guest-free crystals **2** by the vapor adsorption measurements. The guest-binding properties revealed that both guest-free crystals **2** and **3** exhibited the highest adsorption capability for the vapor ethanol and adsorb ethanol and 1-propanol molecules with concomitant guest-induced phase changes. Further studies are focusing on studying crystal structures of thiacalixarenes as other metal complexes and guest adsorption capabilities of the complexes.

Supplementary data

Supplementary data associated with this article can be found in online version at doi:10.1016/j.tet.2011.07.027.

References and notes

1. For example, see (a) Gutsche, C. D. *Calixarenes*; Royal Society of Chemistry: Cambridge, UK, 1989; (b) Vicens, J.; Böhmer, V. In *Calixarenes: A Versatile Class of Macrocyclic Compounds*; Kluwer Academic: Dordrecht, The Netherlands, 1991; (c) Gutsche, C. D. *Calixarenes Revisited*; Royal Society of Chemistry: Cambridge, UK, 1998; (d) Ikeda, A.; Shinkai, S. *Chem. Rev.* **1997**, *97*, 1713–1734; (e) Kim, J. S.; Quang, D. T. *Chem. Rev.* **2007**, *107*, 3780–3799.
2. (a) Kumagai, H.; Hasegawa, M.; Miyanari, S.; Sugawa, Y.; Sato, Y.; Hori, T.; Ueda, S.; Kamiyama, H.; Miyano, S. *Tetrahedron Lett.* **1997**, *38*, 3971–3972; (b) Iki, N.; Kabuto, C.; Fukushima, T.; Kumagai, H.; Takeya, H.; Miyanari, S.; Miyashi, T.; Miyano, S. *Tetrahedron* **2000**, *56*, 1437–1443; (c) Morohashi, N.; Narumi, F.; Iki, N.; Hattori, T.; Miyano, S. *Chem. Rev.* **2006**, *106*, 5291–5316.
3. (a) Katagiri, H.; Iki, N.; Matsunaga, Y.; Kabuto, C.; Miyano, S. *Chem. Commun.* **2002**, 2080–2081; (b) Iki, N.; Morohashi, N.; Yamane, Y.; Miyano, S. *Bull. Chem. Soc. Jpn.* **2003**, *76*, 1763–1768; (c) Kon, N.; Iki, N.; Yamane, Y.; Shirasaki, S.; Miyano, S. *Tetrahedron Lett.* **2004**, *45*, 207–211; (d) Yamada, M.; Shibayama, A.; Kondo, Y.; Hamada, F. *Int. J. Soc. Mater. Eng. Resour.* **2007**, *15*, 13–15; (e) Stoikov, I. I.; Yushkova, E. A.; Zhukov, A. Y.; Zharov, I.; Antipin, I. S.; Konovalov, A. I. *Tetrahedron* **2008**, *64*, 7489–7497; (f) Itoh, S.; Li, C.; Yamada, M.; Akama, M.; Shimakawa, Y.; Kondo, Y.; Hamada, F. *Int. J. Soc. Mater. Eng. Resour.* **2010**, *17*, 211–215.
4. (a) Katagiri, H.; Iki, N.; Hattori, T.; Kabuto, C.; Miyano, S. *J. Am. Chem. Soc.* **2001**, *123*, 779–780; (b) Matsumiya, H.; Ishida, T.; Iki, N.; Miyano, S. *Anal. Chim. Acta* **2003**, *478*, 163–170; (c) Matsumiya, H.; Yasuno, S.; Iki, N.; Miyano, S. *J. Chromatogr., A* **2005**, *1090*, 197–200.
5. (a) Sun, X. H.; Li, W.; Xia, P. F.; Luo, H.-B.; Wei, Y.; Wong, M. S.; Cheng, Y.-K.; Shuang, S. *J. Org. Chem.* **2007**, *72*, 2419–2426; (b) Buie, N. M.; Talanov, V. S.; Butcher, R. J.; Talanova, G. G. *Inorg. Chem.* **2008**, *47*, 3549–3558; (c) Dhir, A.; Bhalla, V.; Kumar, M. *Org. Lett.* **2008**, *10*, 4891–4894; (d) Li, G.-K.; Xu, Z.-X.; Chen, C.-F.; Huang, Z.-T. *Chem. Commun.* **2008**, 1774–1776.
6. (a) Harrowfield, J. M.; Ogden, M. I.; Richmond, W. R.; White, A. H. *J. Chem. Soc., Chem. Commun.* **1991**, 1159–1161; (b) Hamada, F.; Robinson, K. D.; Orr, G. W.; Atwood, J. L. *Supramol. Chem.* **1993**, *2*, 19–24; (c) Davidson, M. G.; Howard, J. A. K.; Lamb, S.; Lehmann, C. W. *Chem. Commun.* **1997**, 1607–1608; (d) Hanna, T. A.; Liu, L.; Zakharov, L. N.; Rheingold, A. L.; Watson, W. H.; Gutsche, C. D. *Tetrahedron* **2002**, *58*, 9751–9757; (e) Thuéry, P.; Asfari, Z.; Vicens, J.; Lamare, V.; Dozol, J.-F. *Polyhedron* **2002**, *22*, 2497–2503; (f) Guillemot, G.; Solari, E.; Rizzoli, C.; Floriani, C. *Chem.—Eur. J.* **2002**, *8*, 2072–2080; (g) Gueneau, E. D.; Fromm, K. M.; Goesmann, H. *Chem.—Eur. J.* **2003**, *9*, 509–514.
7. Bilyk, A.; Hall, A. K.; Harrowfield, J. M.; Hosseini, M. W.; Skelton, B. W.; White, A. H. *Inorg. Chem.* **2001**, *40*, 627–686.
8. Zeller, J.; Radius, U. *Inorg. Chem.* **2006**, *45*, 9487–9492.
9. (a) Endo, K.; Kondo, Y.; Aoyama, Y.; Hamada, F. *Tetrahedron Lett.* **2003**, *44*, 1355–1358; (b) Kondo, Y.; Endo, K.; Hamada, F. *Chem. Commun.* **2005**, 711–712; (c) Yamada, M.; Kondo, Y.; Iki, N.; Kabuto, C.; Hamada, F. *Tetrahedron Lett.* **2008**, *49*, 3906–3911.
10. (a) Yamada, M.; Shimakawa, Y.; Kondo, Y.; Hamada, F. *CrystEngComm* **2010**, *12*, 1311–1315; (b) Yamada, M.; Hamada, F. *CrystEngComm* **2011**, *13*, 2494–2499.
11. (a) Higuchi, Y.; Narita, M.; Niimi, T.; Ogawa, N.; Hamada, F.; Kumagai, H.; Iki, N.; Miyano, S.; Kabuto, C. *Tetrahedron* **2000**, *56*, 4659–4666; (b) Kabuto, C.; Higuchi, Y.; Niimi, T.; Hamada, F.; Iki, N.; Morohashi, N.; Miyano, S. *J. Inclusion Phenom. Macrocyclic Chem.* **2002**, *42*, 89–98; (c) Kasyan, O.; Swierczynski, D.; Drapailo, A.; Suwinska, K.; Lipkowski, J.; Kalchenko, V. *Tetrahedron Lett.* **2003**, *44*, 7167–7170.
12. (a) Kondo, Y.; Endo, K.; Iki, N.; Miyano, S.; Hamada, F. *J. Inclusion Phenom. Macrocyclic Chem.* **2005**, *52*, 45–49; (b) Kondo, Y.; Hamada, F. *J. Inclusion Phenom. Macrocyclic Chem.* **2007**, *58*, 123–126.
13. Sheldrick, G. M. *SHELXS-97 Program for Solution of Crystal Structures*; University of Göttingen: Germany, 1997.
14. Sheldrick, G. M. *SHELXL-97 Program for Refinement of Crystal Structures*; University of Göttingen: Germany, 1997.